

Research Article

Pickling Behaviour of 2205 Duplex Stainless Steel Hot-rolled Strips in Sulfuric Acid Electrolytes

Jianguo Peng ^{1,2}, Moucheng Li ^{1*}

¹ Institute of Materials, Shanghai University, Shanghai 200072, China;

² Research Institute, Baoshan Iron & Steel Co., Ltd., Shanghai 200431, China

Correspondence should be addressed to Jianguo Peng; peng_jianguo@baosteel.com and Moucheng Li; mouchengli@shu.edu.cn

Received 9 October 2019; Revised 8 March; Accepted 17 March

Academic Editor :

Copyright ©2019 Jianguo Peng et al. This is an open access article distributed under the Creative Commons Attribution License, which permits unrestricted use, distribution, and reproduction in any medium, provided the original work is properly cited.

Pickling behaviour of the oxide layer on hot-rolled 2205 duplex stainless steel (DSS) was studied in H₂SO₄ solutions with electrolytic workstation. The pickling rate at 75 °C increases slightly with the H₂SO₄ concentration from 100 to 250 g L⁻¹, but increases markedly as the concentration is higher than 250 g L⁻¹. The solution temperature greatly accelerates the pickling rate. Fe³⁺ ion is an effective oxidant, which shows stronger inhibitive effect. The rotating disk electrode was used to simulate the moving state of steel strips in practice. The movement with the speed from 0 to 20 m min⁻¹ results in weak acceleration effect on the pickling process. Under dynamic conditions, the pickling rate increases noticeably with changing the pulse current density from 0 to 0.2 A cm⁻². The industrial pickling efficiency of 2205 DSS hot-rolled strips increases from 5-8 m/min to 15-18 m/min. The surface quality is improved.

1. Introduction

Type 2205 duplex stainless steel (DSS) has been used widely in many industries for its excellent mechanical properties and corrosion resistance [1-6]. However, the oxide scales formed on the surface of 2205 DSS during rolling and heat treatment are stable and dense due to the high chromium, molybdenum and nitrogen contents [7]. Moreover, oxide nodules may often grow on the surface of 2205 DSS for the different oxidation rates of ferritic and austenitic phases at high temperature [8-9]. Therefore, the pickling of 2205 DSS hot-rolled strips is more difficult than that of standard austenitic grades [10].

The pickling process of stainless steels is used to remove the oxide scales and chromium depleted layer in order to restore the corrosion resistance and ensure the surface finish [11-12]. The industrial pickling process includes mechanical descaling, pre-pickling, and mixed-acid pickling. A mechanical descaling is achieved through breaking, grinding, roto blasting, and sand blasting processes. Pre-pickling is performed either anodically or cathodically in acid or neutral electrolytes with certain current densities [13-15]. The general electrolytes are Na₂SO₄, H₂SO₄, H₃PO₄, HCl, HF and H₂O₂. Mixed-acid pickling is the final step to dissolve the oxide scales in H₂SO₄-HF [16], H₃PO₄-H₂SO₄ [17], HCl-HF [18] or HNO₃-HF [19].

Pre-pickling plays a critical role for the industrial production process of 2205 DSS hot-rolled strips. Na₂SO₄

electrolytes can conduct electricity, but they cannot dissolve the oxides and matrix [20]. H_2SO_4 solutions can dissolve the oxide scales and matrix [16, 21]. H_3PO_4 solutions have good properties of dissolving oxide scales, but their cost are expensive [22]. HCl solutions can dissolve ferrous oxides, but chloride corrosion is the big problem [18, 23-25]. HF solutions can dissolve oxide scales and SiO_2 , but there is a serious intergranular corrosion problem [16,18]. The dissolving effect of H_2O_2 is remarkable on the Cr-depleted layer of stainless steel, but unsatisfactory on the oxide scale [26-27]. After comparison, H_2SO_4 solutions are extensively used in practice for their low cost and chemical stability.

Pickling process can be simulated with static and dynamic conditions at the laboratories. There are many studies on static pickling [16-26], but very few on dynamic pickling [22]. The stainless steel strips in the industrial pickling process is moving. So the studies focused on dynamic pickling are of practical significance.

The pickling technology and mechanism are well known for the austenitic and ferritic stainless steels in the literature, but there are few systematical reports focused on the pickling for duplex stainless steel, especially for DSS 2205 hot-rolled strips. With the rapid development of economy and living standard, the demand for 2205 DSS is increasing quickly. However, the production of 2205 DSS is restricted greatly by its pickling process. It is necessary to study the pickling laws and improve the pickling efficient for 2205 DSS hot-rolled strips. In this work, the pickling behaviour of 2205 DSS hot-rolled strip in H_2SO_4 electrolytes under both static and dynamic conditions was investigated. The pickling mechanism was discussed on the basis of mass loss and surface analysis.

2. Experimental

2.1 Materials. A hot-rolled 2205 duplex stainless steel strip with a thickness of 4.0 mm was used as the test materials. Its chemical composition is given in table 1.

TABLE 1. Chemical composition of 2205 DSS specimens (wt. %)

C	Si	Mn	S	P	Cr	Ni	Mo	N
0.024	0.62	1.42	0.001	0.024	21.13	5.46	3.11	0.15

2.2 Sample Preparation. A plate of 300×300 mm was cut from the strip and annealed at 1140 °C for 4 min. After annealing, the plate was taken out from the furnace and cooled down in air. The annealed plate was subjected to sand blasting to remove its main oxides on the surface and then was cut into test specimen of 5×5 mm. The specimens were covered with epoxy resin leaving a working area of 5×5 mm and cleaned with alcohol before pickling.

2.3 Pickling Measurement. Pickling tests were carried out on the workstation as shown in Figure 1. A specimen fixed on the rotating disk with a diameter of 15 cm was used as working electrode, a platinum sheet as counter electrode, and Hg/Hg_2SO_4 as reference electrode. The analytically pure H_2SO_4 , ferrous sulfate, iron sulfate and de-ionized water were used to prepare the electrolytes. The pickling processes were performed with a Princeton potentiostat (PAR 273A).

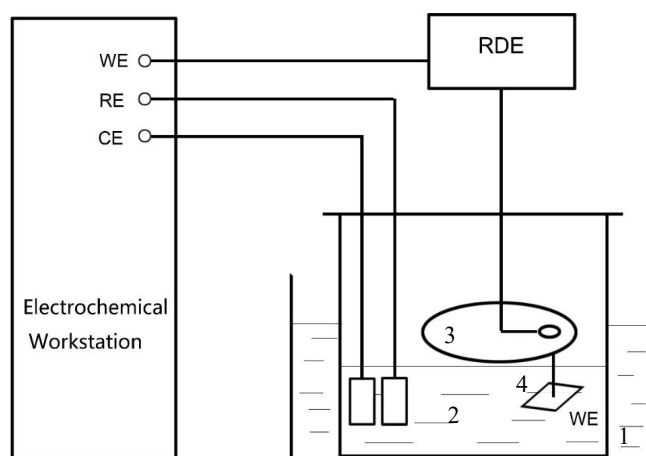


FIGURE 1: Electrolytic workstation used for dynamic pickling tests.
1-thermostat water bath, 2-electrolyte, 3- rotating disk, 4-specimen

2.4 Electrochemical measurement. The corrosion potential and electrochemical impedance spectroscopy (EIS) of the test specimens were measured during the pickling process with a Princeton potentiostat (VMP3). Each specimen was fixed on the cell sidewall with a 1 cm² round hole. The test specimen was used as the working electrode; the platinum sheet was used as the counter electrode; and the Hg/Hg₂SO₄ was used as the reference electrode (MSE).

All test samples were immersed in the electrolytes for 2 min. During electrolysis, the electrolytic time was 81 seconds with three periods. For each period, the specimen was polarized anodically for 18 seconds and cathodically for 9 seconds at various current densities. The pickling rate was calculated from the mass loss of specimen with a precision of 0.01 mg. The specimens were characterized with scanning electron microscopy (FEI, quanta 600) and Roman spectroscopy (Renishaw, INVIA).

3. Results

3.1 Characterization of oxide scales.

In general, the oxide scale of hot-rolled 2205 DSS strip after annealing can be divided into an inner layer and an outer layer[7]. Chromium is rich in the inner layer while iron is rich in the outer layer. The outer layer is consisted of Fe₂O₃, Fe₃O₄ and FeCr₂O₄ and the inner layer is composed mainly of FeCr₂O₄ [28]. The outer layer may be partially removed by mechanical descaling. The FeCr₂O₄ is the oxide with a spinel structure, which is insoluble in most industrial acids[7,29].

As shown in the Figure 2, a few oxide scales remain on the surface of test specimen after shot blasting. Roman spectrum in Figure 3 indicates that the residual oxides on the surface of 2205 DSS hot-rolled strip are composed of Fe₂O₃, Fe₃O₄ and FeCr₂O₄. Among them, the content of FeCr₂O₄ is the highest as seen from its peak intensity. This implies that the pickling of 2205 DSS hot-rolled strip is difficult.

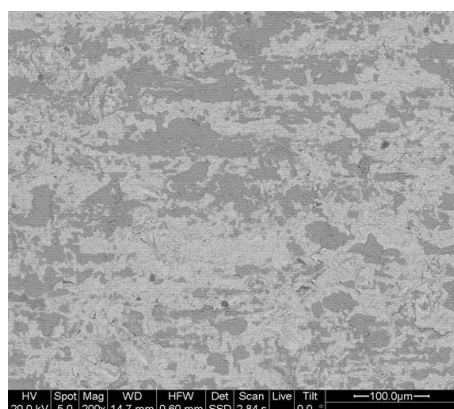


FIGURE 2: Surface image for the test specimen

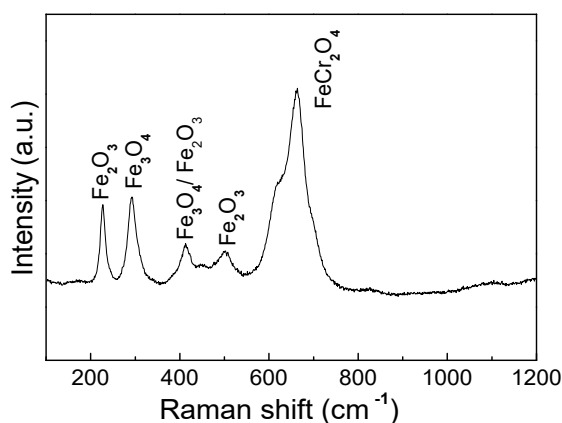


FIGURE 3: Roman spectrum for the test specimens

3.2 Chemical pickling properties under static condition.

The static chemical pickling of stainless steel in H₂SO₄ solutions is mainly related with acid concentration, pickling temperature and concentration of metal ions. For most steels, higher pickling temperature, higher concentration of H₂SO₄ solutions and lower concentration of metal ions can improve its pickling efficiency in initial pickling stage for its strong dissolving capacity. After pickling for a certain time, the strong dissolving capacity may deteriorate pickling result for the corrosion of matrix.

The effect of H₂SO₄ concentration on static pickling rate and typical surface images of specimens at 75 °C are shown in Figures 4 and 5. The pickling efficiency has a positive correlation with H₂SO₄ concentration. It can be seen that the pickling rate has a transition at about 250 g L⁻¹. When the concentration increases from 100 g L⁻¹ to 250 g L⁻¹, the pickling rate is accelerated slightly and many oxide scales remain on the surface. When the concentration increases from 250 g L⁻¹ to 450 g L⁻¹, the pickling rate is accelerated markedly to remove most of the oxide scales.

Figure 6 gives the static pickling rates of specimens in 300 g L⁻¹ H₂SO₄ solutions at different temperatures. The pickling efficiency has a positive correlation with the solution temperature. With increasing temperature from 50 °C to 90 °C, the pickling rate increases gradually from about 1.74 to 12.8 g m⁻² min⁻¹ and the retained oxide scales reduced noticeably, as shown in Figure 7.

The metal ions in the H₂SO₄ solutions include iron, chromium, molybdenum, nickel, manganese, titanium and niobium ions. The conventional metal elements in industrial H₂SO₄ electrolytes are shown in table 2. Among them, iron is the main element. So the iron ions play the main impact on the pickling process.

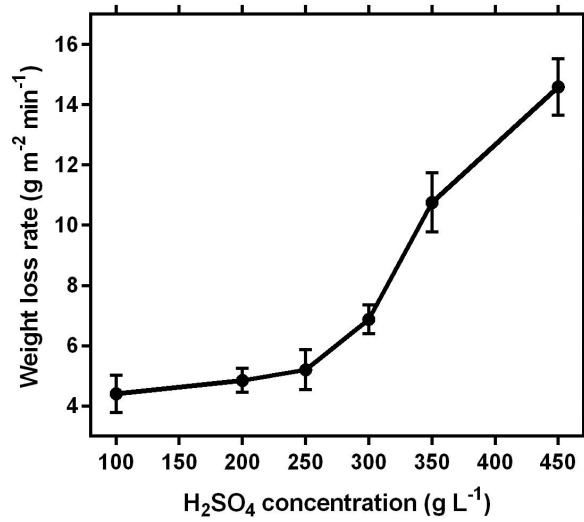


FIGURE 4: Variation of static pickling rate in H₂SO₄ at 75 °C with different concentration

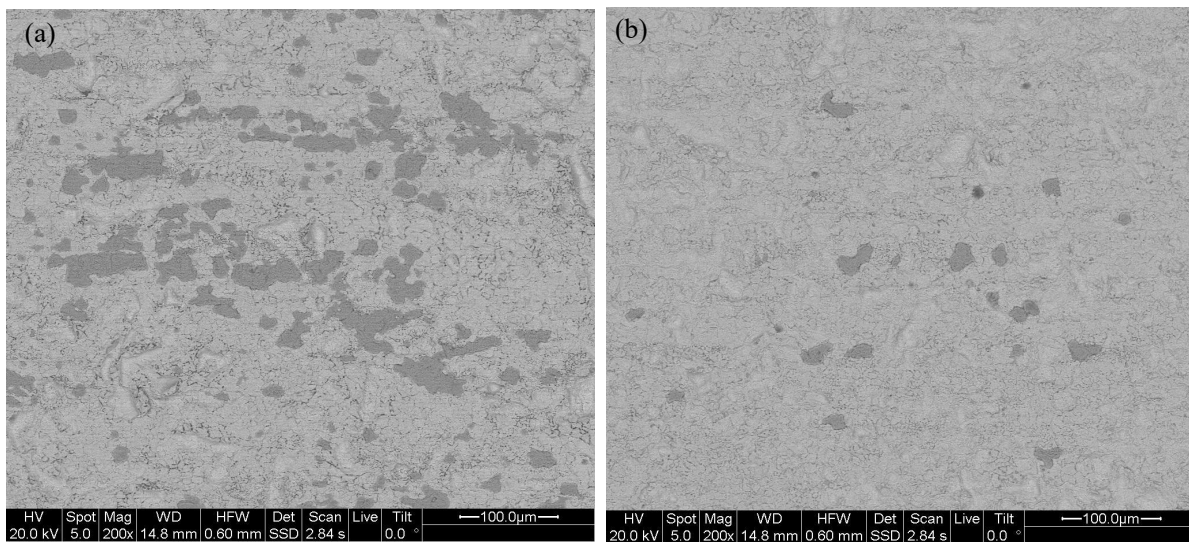


FIGURE 5: SEM surface images after static pickling in H₂SO₄ solutions at 75 °C with different concentrations (a) 300 g L⁻¹ and (b) 450 g L⁻¹.

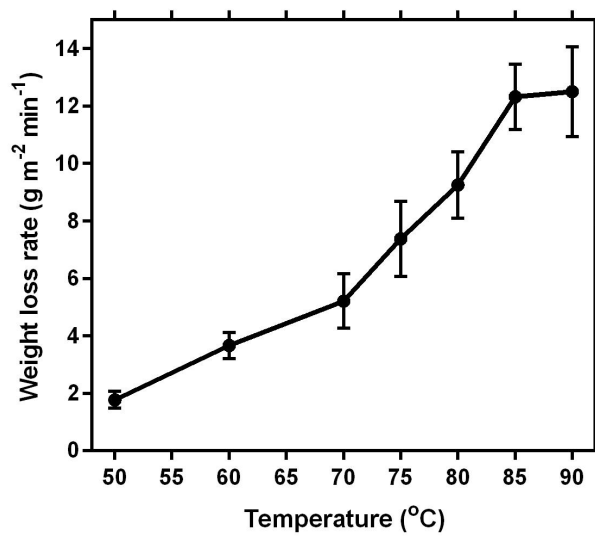


FIGURE 6: The static pickling rate of specimen in 300 g L⁻¹ H₂SO₄ solutions at different temperatures

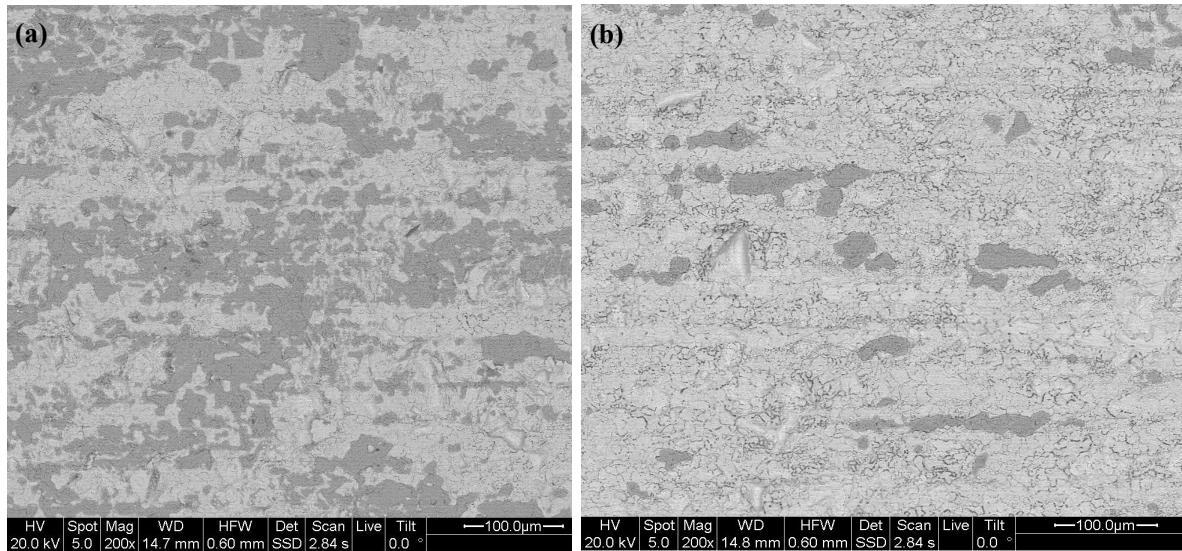


FIGURE 7. SEM surface images after static pickling in 300 g L⁻¹ H₂SO₄ solutions at temperatures 60 °C (a) and 90 °C (b).

TABLE 2. Concentration of metal ions in industrial H₂SO₄ solutions

Ions	Fe	Cr	Mn	Ni	Cu	Nb	Ti	Mo
Concentration (g/L)	20.6	2.80	0.06	0.55	<0.01	<0.01	<0.01	0.04

The effect of iron ions on the static pickling of specimen was studied in 300 g L⁻¹ H₂SO₄ solutions at 75 °C and the results are given in Figure 8. The pickling efficiency has a negative correlation with concentration of iron ions. With increasing concentration of ferric ions from 0.5 g L⁻¹ to 60 g L⁻¹, the pickling rate declines sharply at first to less than 1 g m⁻² min⁻¹ and then decreases insignificantly. With increasing concentration of ferrous ions, the pickling rate decreases slowly, but shows higher values in comparison with ferric ions. The ferric ions are an effective oxidant which can enhance the corrosion potential of test specimens [16], then reduce their dissolution rate remarkably. In order to improve the pickling rate of 2205 DSS hot-rolled strips, new sulfuric acid solutions without iron ions are necessary.

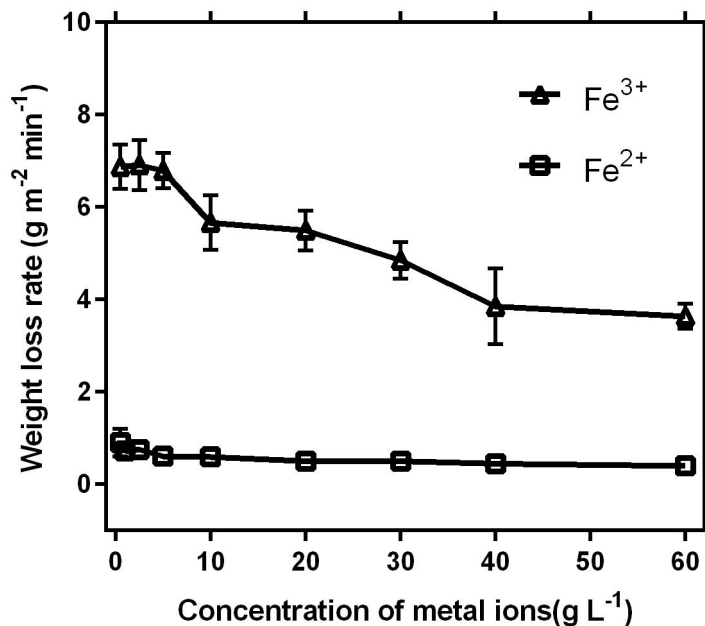


FIGURE 8. The static pickling rate in 300 g L⁻¹ H₂SO₄ solutions at 75 °C with different iron ions

3.3 Chemical pickling properties under dynamic conditions.

In order to see the difference between dynamic and static pickling of hot-rolled 2205 DSS strips, the rotating disk was applied to create the movement between specimens and acid solutions. The variation of pickling rate of specimen in 300 g L⁻¹ H₂SO₄ solutions at 75 °C with rotary speed is given in Figure 9. The pickling efficiency has a positive correlation with moving speed of specimen. The pickling rate is higher in the dynamic cases than in the static case. However, with the increase of rotary speed from 5 to 20 m min⁻¹, the pickling rate only enlarges slightly from about 7.5 to 7.8 g m⁻² min⁻¹. It is evident that the acceleration effect of dynamic speed is very weak.

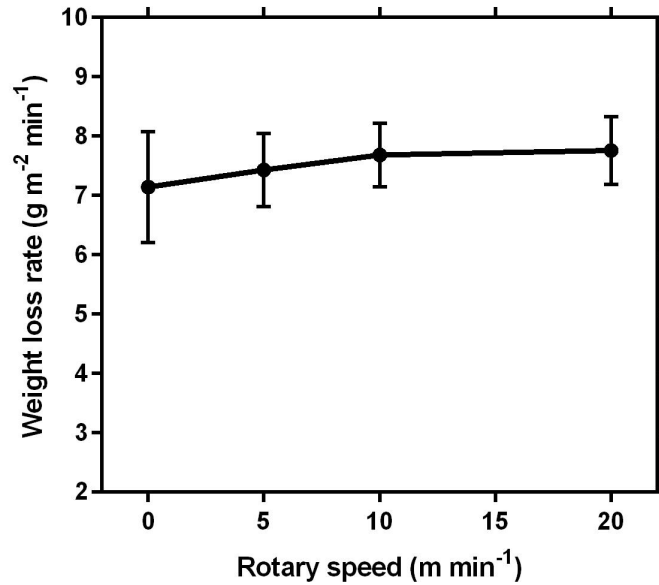


FIGURE 9: Dynamic pickling rate in 300 g L⁻¹ H₂SO₄ solutions at 75 °C under different rotary speed conditions

3.4 Electrolytic pickling properties under dynamic condition.

The applied polarization plays a role in pickling process. Figure 10 gives the variation of dynamic pickling rate at 10 m min⁻¹ for specimens in 300 g L⁻¹ H₂SO₄ solutions at 75 °C with pulse current density. The pickling rate becomes higher with increasing the pulse current density from 0 to 0.2 A cm⁻². The rate is about 2.1 times larger at 0.2 A cm⁻² than at 0 A cm⁻² (i.e., the chemical pickling). The electrolytic pickling efficiency has a positive correlation with the pulse current density. After dynamic electrolytic pickling, there is almost no oxide scales on the specimen surfaces compared with static electrolytic pickling. With the increase of current density from 0.04 A cm⁻² to 0.2 A cm⁻², the Cr-depleted layer may dissolve obviously and the surfaces become smooth, as shown in Figure 11.

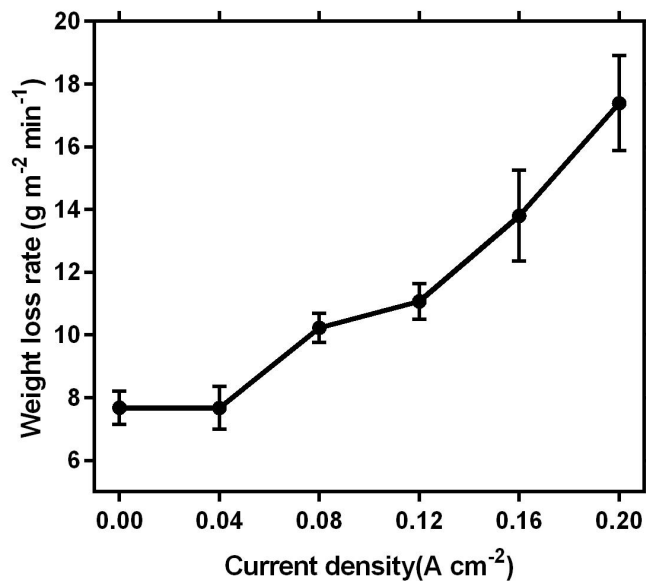


FIGURE 10: Variation of dynamic pickling rate with current density in 300 g L⁻¹ H₂SO₄ solutions at 75 °C

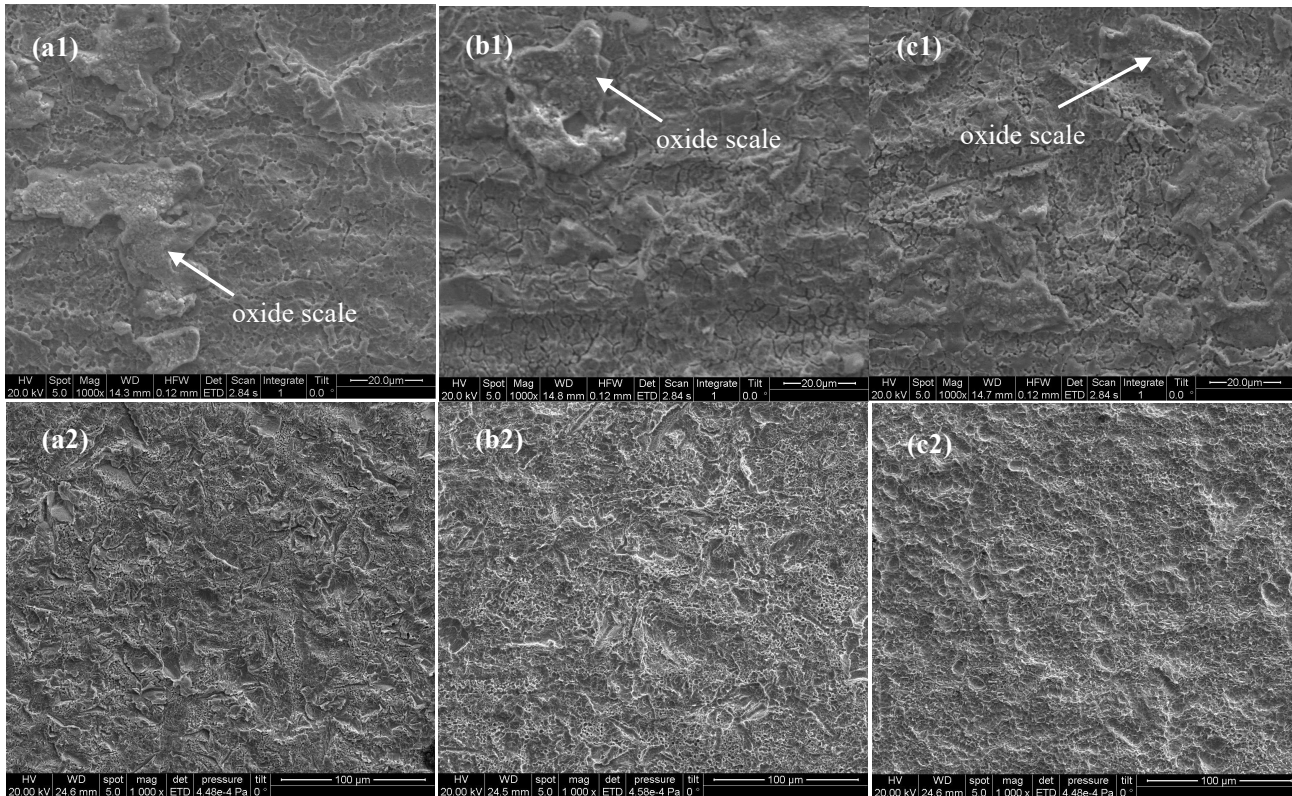
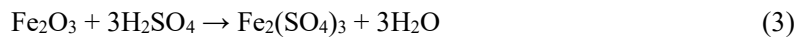
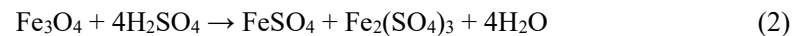


FIGURE 11: SEM surface images after static (a1,b1,c1) and dynamic (a2,b2,c2) pickling in 300 g L⁻¹ H₂SO₄ solutions at 75 °C with current density 0.04 A cm⁻² (a1,a2) , 0.12 A cm⁻² (b1,b2) and 0.2 A cm⁻² (c1,c2).

4. Discussion

The residual oxides on the surface of test specimen are composed of Fe₂O₃, Fe₃O₄ and FeCr₂O₄ as shown in Figure 3. While pickling of 2205 DSS hot-rolled strips in H₂SO₄ electrolytes, it involves two processes, chemical pickling process and electrolytic pickling process.

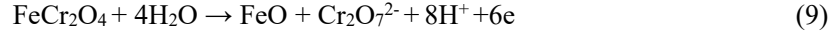
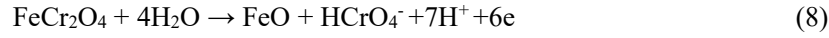
When chemical pickling is carried on for 2205 DSS, FeO, Fe₂O₃, Fe₃O₄ and alloying elements can be dissolved in H₂SO₄ solutions. The chemical pickling process involves the following chemical reactions [30].



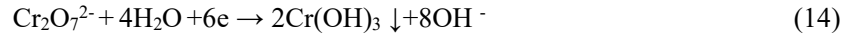
The oxide scales on the test specimen are mainly comprised of FeCr₂O₄ as shown in Figure 3. The FeCr₂O₄ is insoluble in sulfuric acid solution [7]. The matrix of 2205 DSS is dissolved slowly in sulfuric acid solution for its excellent corrosion resistance. The oxide scales on the test specimen is dissolved very slowly in sulfuric acid solutions by mean of peeling mechanically. So the chemical pickling of 2205 DSS hot-rolled strip is very slowly. For most stainless steels, higher pickling temperature and sulfuric acid concentration do not increase their pickling efficiency after a certain level [30]. But for 2205 DSS, the oxide scales are still existed after chemical pickling in 450 g L⁻¹ H₂SO₄ at 90 °C.

At the beginning of static chemical pickling process, small gas bubbles nucleate and grow on the specimen surface. During the pickling process, more and more gas bubbles will form and adsorb on the specimen surface, which must reduce the contact areas of effective pickling. As for the dynamic pickling of specimens on the rotating disk, the movement may decrease the adsorption and growth of gas bubbles on the specimen surface to a certain extent [31]. So the chemical pickling rate of the annealed 2205 DSS specimens under dynamic condition is higher than under static condition. Nevertheless, the acceleration effect of dynamic speed is very weak, with about 5~10% increase in the pickling rates as observed in Figure 8.

When sulfuric acid is used as electrolyte, it can conduct electricity. The test specimen serves as anode and cathode with the alternative change. When the test specimen serves as the relative anode, the insoluble FeCr_2O_4 is oxidized into soluble HCrO_4^- and $\text{Cr}_2\text{O}_7^{2-}$. The anodic electrolytic reactions are as followed [10,30,32].



When the test specimen serves as the relative cathode, $\text{Cr}(\text{OH})_3$ and $\text{Fe}(\text{OH})_3$ are deposited on the surface of test specimen. H_2 is precipitated between the oxide layers, which is beneficial to the separation of the deposit sediment from the matrix. The cathodic electrolytic reactions are as followed [10,30,32].



Electrolytic pickling is faster than normal chemical pickling for most stainless steels [20]. The electrolytic pickling process in H_2SO_4 electrolytes is the combined effect of electrolysis and chemical pickling. When the electrolytic pickling is performed under static conditions, a maximum of about 20% of the current goes to dissolution reactions whereas about 80% of the current is consumed in oxygen gas production [10]. For the dense and compact oxide scales of the test specimens, spallation or peeling of the oxide scales induced by gas evolution does not play a decisive role. As shown in Figure 11, the oxide scales are remained on the test specimens after static electrolytic pickling. When the electrolytic pickling is performed under dynamic conditions, the rotary disk develops a rational way for producing active edges efficiently, where catalytic activity of the test specimens is improved and its pickling rate is accelerated [33-34]. The dynamic electrolytic pickling rate at 0.2 A cm^{-2} is about 2.1 times higher than the chemical pickling, which may give rise to a smooth specimen surface without oxide scales.

The Fe^{3+} ions are an effective oxidant which enhanced the corrosion potential, as shown in Figure 12. When none Fe ions were added in the H_2SO_4 solutions, the corrosion potential quickly declined at the beginning of the immersion time, after about 50 s, it remained constant (approximately $-0.75 \text{ V}_{\text{MSE}}$) subsequently as the immersion time increased. When $10 \text{ g L}^{-1} \text{ Fe}^{2+}$ was added in the H_2SO_4 solutions, the corrosion potential quickly declined at the beginning of the immersion time, after about 100s, it remained unchanged. When $10 \text{ g L}^{-1} \text{ Fe}^{3+}$ was added in the H_2SO_4 solutions, the corrosion potential increased slowly from $0.062 \text{ V}_{\text{MSE}}$ to $0.137 \text{ V}_{\text{MSE}}$ as the immersion time increased. The EIS Nyquist plot recorded on the test specimens immersed in $300 \text{ g L}^{-1} \text{ H}_2\text{SO}_4$ solutions containing none ions, $10 \text{ g L}^{-1} \text{ Fe}^{2+}$, $10 \text{ g L}^{-1} \text{ Fe}^{3+}$ under the E_{corr} conditions (i.e., the free corrosion states) is presented in Figure 13. The semicircle size enlarged slightly with the addition of $10 \text{ g L}^{-1} \text{ Fe}^{2+}$, but increased noticeably with the addition of the $10 \text{ g L}^{-1} \text{ Fe}^{3+}$ for its high impedance.

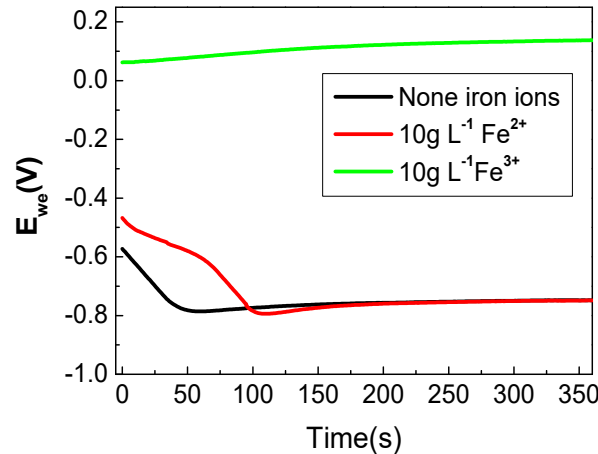


FIGURE 12. Corrosion potential in $300 \text{ g L}^{-1} \text{ H}_2\text{SO}_4$ solutions at $75 \text{ }^\circ\text{C}$ containing different Fe ions

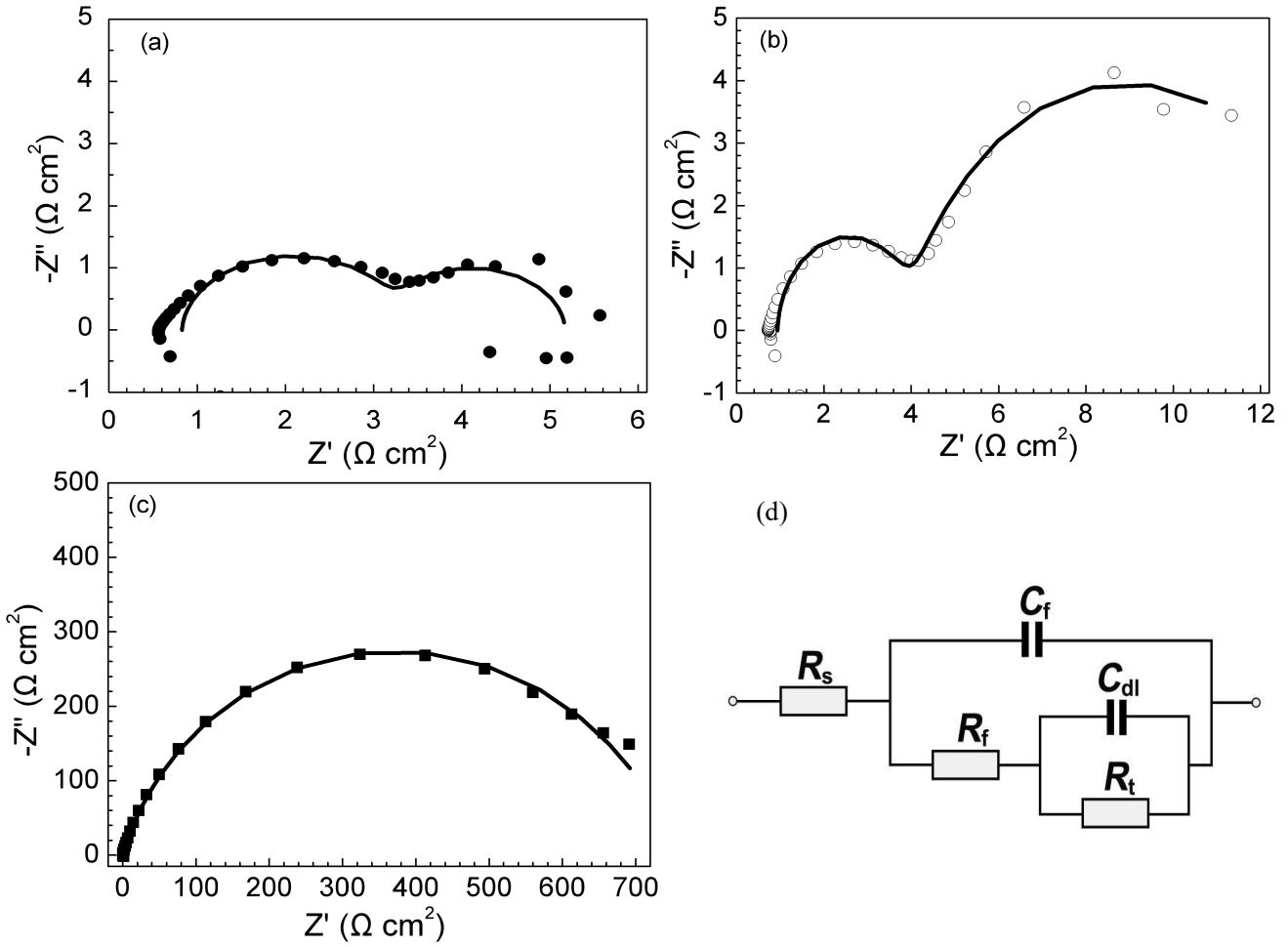


FIGURE 13: Nyquist plots (a,b,c) in 300 g L⁻¹ H₂SO₄ solutions at 75 °C containing none ions (a), 10 g L⁻¹ Fe²⁺ (b), 10 g L⁻¹ Fe³⁺ (c), and the corresponding circuit of the impedance spectrum (d)

In order to show the dissolution process for the specimens in 300 g L⁻¹ H₂SO₄ solutions at 75 °C containing different Fe ions, the equivalent circuit model is proposed in Figure 13 (d) according to the EIS features in Figure 13. R_s is the electrolyte resistance. R_f is the resistance of oxide layer remained on the specimens. R_t is the charge transfer resistance. C_f and C_{dl} can be replaced with constant phase element (CPE) [35]. The impedance of CPE is written in equation (15), where Y_0 is the admittance magnitude of CPE, α is the exponential term. Table 3 gives the fitted results of EIS spectra. The calculated spectra are shown as a solid curve in Figure 13, which fit the experimental data very well. It can be concluded that the model provided a reliable description for the corrosion systems.

$$Z_{CPE} = \frac{1}{Y_0(j\omega)^\alpha} \quad (15)$$

TABLE 3: Fitted results for EIS spectra in 300 g L⁻¹ H₂SO₄ solutions at 75 °C containing different ions

ions	R_s $\Omega \text{ cm}^2$	Y_{0-f} $S^\alpha \Omega^{-1} \text{ cm}^{-2}$	α_f	R_f $\Omega \text{ cm}^2$	Y_{0-dl} $S^\alpha \Omega^{-1} \text{ cm}^{-2}$	α_{dl}	R_t $\Omega \text{ cm}^2$
None ions	0.82	0.00218	0.87	2.80	0.0658	0.92	1.6
10g L ⁻¹ Fe ²⁺	0.94	0.00185	0.96	3.14	0.093	0.84	10
10g L ⁻¹ Fe ³⁺	1.04	0.000133	0.95	54.99	0.000281	0.68	70.6

5. Application and performance

According to the above results, the pickling process of hot-rolled 2205 DSS is optimized through the high H₂SO₄ concentration, high solution temperature and proper electrolysis current density in the industrial pre-pickling of

2205 DSS hot-rolled strips. The pickling efficiency is improved remarkably, which increases the production rate from 5–8 m min⁻¹ to 15–18 m min⁻¹. Besides, the surface finish after pickling is notably enhanced, as shown in Figure 14.



FIGURE 14: Optical surface of 2205 DSS hot-rolled strip after industrial pickling with optimized pickling process

6. Conclusions

The pickling behaviour of hot-rolled 2205 DSS with annealing and mechanical descaling treatments in H₂SO₄ solutions under both static and dynamic conditions has led to the following conclusions:

(1) In static chemical pickling process, the pickling rate may be accelerated noticeably by increasing the solution temperature and H₂SO₄ concentration, but be decelerated greatly by Fe³⁺ ions.

(2) The chemical pickling process can be enhanced weakly by the moving speed of specimen from 0 to 20 m min⁻¹ because the movement decreases the adsorption and growth of gas bubbles on the specimen surface to a certain extent.

(3) Under dynamic conditions, the electrolytic pickling rate increases markedly with changing the pulse current density from 0.04 to 0.2 A cm⁻². The electrolytic pickling rate at 0.2 A cm⁻² is about 2.1 times larger than the chemical pickling rate in 300 g L⁻¹ H₂SO₄ at 75 °C, resulting in the smooth and clean specimen surfaces.

Data Availability

The tables and figures data used to support the findings of this study are available from the corresponding authors on reasonable request.

Conflict of Interests

The authors declare that there is no conflict of interests regarding the publication of this paper.

Acknowledgments

Financial support from National Natural Science Foundation of China (Grant Nos. U1660205 and U1960103) is gratefully acknowledged.

References

- [1] Y. -Y. Wu, P. -M. Francisco, “Chloride Levels That Initiated Corrosion of Duplex Stainless Steel Embedded in Mortar,” *Advances in Materials Science and Engineering*, vol. 2019, pp. 1-6, 2019.
- [2] T. Q. Li, Y. Y. Zhang, L. Gao, Y. H. Zhang, “Optimization of FCAW Parameters for Ferrite Content in 2205 DSS Welds Based on the Taguchi Design Method,” *Advances in Materials Science and Engineering*, vol. 2018, pp. 1-7, 2018.
- [3] Q. Meng, P. Q. La, L. Yao et al., “Effect of Al on Microstructure and Properties of Hot-Rolled 2205 Dual Stainless Steel,” *Advances in Materials Science and Engineering*, vol.2016, pp.1-8, 2016.
- [4] Z. G. Song, H. Feng, S. M. Hu, “Development of Chinese duplex stainless steel in recent year,” *Journal of Iron and Steel Research*, vol.2, pp. 121-131, 2017.
- [5] Z. Y. Liu, C. F. Dong, X. G. Li, et al., “Stress corrosion of 2205 duplex stainless steel in H₂S-CO₂

- environment,” *Journal of Materials Science*, vol. 44, no. 16, pp. 4228-4234, 2009.
- [6] R. N. Gun, “Duplex Stainless Steels,” Abington Publishing, Cambridge, pp.1, 1994.
- [7] L. -F. Li, Z. H. Jiang, Y. Riquier, “High-temperature oxidation of duplex stainless steels in air and mixed gas of air and CH₄,” *Corrosion Science*, vol. 47, pp. 57–68, 2005.
- [8] J. G. Peng, M. C. Li, S. Z. Luo et al., “Oxidation characteristics of duplex stainless steel 2205 in simulated combustion atmosphere,” *Materials Research Innovation*, vol. suppl 5, pp. 245-249, 2015.
- [9] J. G. Peng, M. C. Li, “High Temperature Oxidation behaviour of DSS2205 in humid Air,” *Advanced Materials Research*, vol. 900, pp. 673-676, 2014.
- [10] N. Ipek, B. Holm, R. Pettersson et al., “Electrolytic pickling of duplex stainless steel,” *Materials Corrosion*, vol. 56, no. 8, pp. 521-532, 2005.
- [11] J. G. Peng, S. Z. Luo, W. B. Dong. “Study on the simulated pickling of 443NT medium chrome ferritic stainless steel,” *Baosteel Technical Research*, vol.4, no.1, pp50-52, 2010.
- [12] L. -F. Li, M. Daerden, P. Caenen et al., “Electrochemical behaviour of Hot-Rolled 304 Stainless Steel during Chemical Pickling in HCl-Based Electrolytes,” *Journal of Electrochemical Society*,” vol. 153, no. 5, pp. B145-B150, 2006.
- [13] J. Hildén, J. Virtanen, O. Forsén et al., “Electrolytic pickling of stainless steel studied by electrochemical polarisation and DC resistance measurements combined with surface analysis,” *Electrochimica Acta*, vol. 46, no. 24, pp. 3859-3866, 2001.
- [14] L. Li, P. Caenen, M. Jiang, “Electrolytic pickling of the oxide layer on hot-rolled 304 stainless steel in sodium sulphate,” *Corrosion Science*, vol. 50, no. 10, pp. 2824-2830, 2008.
- [15] W. G. Chen, Y.Q. Chen, H.L. Pang, “Study of Na₂SO₄ electrolytic pickling process on 304 stainless steel,” *China Metallurgy*, vol. 19, no. 1, pp. 16-23, 2009.
- [16] L. -F. Li, P. Caenen, J.P. Celis, “Chemical Pickling of 304 stainless steel in Fluoride- and sulfate-Containing Acidic Electrolytes,” *Journal of The Electrochemical Society*, vol. 152, no. 9, pp. B352-357, 2005.
- [17] C. A. Huang, C. C. Hsu, “The electrochemical polishing behaviour of duplex stainless steel (SAF 2205) in phosphoric-sulfuric mixed acids,” *International Journal of Advance Manufacture Technology*, vol. 34, no. 9-10, pp. 904-910, 2007.
- [18] L. -F. Li, P. Caenen, M. Daerden et al., “Mechanism of single and multiple step pickling of 304 stainless steel in acid electrolytes,” *Corrosion Science*, vol. 47, pp. 1307-1324, 2005.
- [19] B. S. Covino, J. V. Scalera, J. J. Driscoll et al., “Dissolution behaviour of 304 stainless steel in HNO₃/HF mixtures,” *Metallurgical Transactions A*, vol. 17, no. 1, pp. 137–149, 1986.
- [20] N. Ipek, N. Lior, M. Vynnycky et al., “Numerical and experimental study of the effect of gas evolution in electrolytic pickling,” *Journal of Applied Electrochemistry*, vol. 36, pp. 1367- 1379, 2006.
- [21] M. Abdallah, “Guar gum as corrosion inhibitor for carbon steel in sulfuric acid solutions,” *Portugaliae Electrochimica Acta*, vol. 22, no. 2, pp. 161–175, 2004.
- [22] C. A. Huang, J. H. Chang, W. J. Zhao et al., “Examination of the electropolishing behaviour of 73 brass in a 70% H₃PO₄ solution using a rotating disc electrode,” *Materials Chemistry and Physics*, vol. 146, no. 3, pp. 230-239, 2014.
- [23] Q. Xie, P. Y. Shi, C. J. Liu et al., “Effects of Different Oxidants on HCl-based Pickling Process of 430 Stainless Steel,” *Journal of Iron and Steel Research*, vol. 8, pp. 778-784, 2016.
- [24] W. H. Hao, L.Y. Qin, D. L. Liu, “The effect of hydrochloric acid concentration on pickling of duplex stainless steel,” *Corrosion Protection*, vol. 33, no. suppl 2, pp: 69-71, 2012.
- [25] H. Y. Li, A. C. Zhao, “Pickling behaviour of Duplex Stainless Steel 2205 in Hydrochloric Acid Solution,” *Advances in Materials Science and Engineering*, vol. 2018, pp. 1-6, 2018.
- [26] C. J. Brown, “Process and apparatus for recovery of peroxide containing pickling solutions,” *International Patent*, PCT/CA02/01598, 24 Oct 2002.
- [27] R.Y. Jiang, G. B. Zou, W. Shi et al., “Corrosion behaviour of Plasma-Nitrided 904L autenitic stainless steel in hydrofluoric acid,” *Journal of Materials Engineering and Performance*, vol. 28, no. 3, pp. 1863-1872, 2019.
- [28] Č. Donik, A. Kocijan, J.T. Grant et al.. “ XPS study of duplex stainless steel oxidized by oxygen atoms,” *Corrosion Science*, vol. 51, pp. 827-832, 2009.
- [29] Y. X. Xu, Q. Jin, J. Li et al., “Oxidation induced phase transformation of duplex stainless steel 25Cr-10Mn-2Ni-3Mo-0.8W-0.5N,” *Corrosion Science*, vol. 55, pp. 233-237, 2012.
- [30] ASM Handbook Committee. “ASM Handbook Volume 5 Surface Engineering,” ASM International, 2007.
- [31] J. Eigeldinger, H. Vogt, “The bubble coverage of gas-evolving electrodes in a flowing electrolyte,” *Electrochimica Acta*, vol. 45, no. 27, pp. 4449-4456, 2000.
- [32] M. Pourbaix, *Atlas of electrochemical equilibria in aqueous solutions*, second ed., Pergamon Press, Oxford, 1966.

- [33] Z. G. Wang, H. -H. H. Wu, Q. Li et al., "Reversing Interfacial Catalysis of Ambipolar WSe₂ Single Crystal," *Advanced Science*, vol.7, no. 1901382, pp. 1-9, 2019.
- [34] Z. G. Wang, Q. Li, H. X. Xu et al., "Controllable etching of MoS₂ basal planes for enhanced hydrogen evolution through the formation of active edge sites," *Nano Energy*, vol. 49, pp. 634-643, 2018.
- [35] M. C. Li, C. L. Zeng, S. Z. Luo et al., "Electrochemical corrosion characteristics of type 316 stainless steel in simulated anode environment for PEMFC," *Electrochimical Acta*, vol. 48, pp. 1735-1741, 2003.